

Thin-cell dielectric response of a ferroelectric liquid crystal

R. J. Cava, J. S. Patel, K. R. Collen, J. W. Goodby, and E. A. Rietman

AT&T Bell Laboratories, Murray Hill, New Jersey 07974-2070

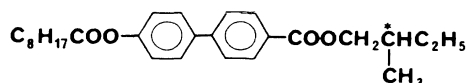
(Received 23 October 1986)

The results of a study of the dielectric response of the liquid crystal BOH8-MPOOBC in the frequency range 5 Hz to 13 MHz, in the vicinity of the phase transition to the ferroelectric phase, in an aligned cell of $2.7 \mu\text{m}$ thickness, are presented. At small ac probe fields, critical-like behavior is observed in the dielectric permittivity and the characteristic relaxation time of molecules in the bulk of the sample. At high ac probe fields, a second relaxation appears due to the reorientation of molecules at the cell surfaces. The dielectric strength of the bulk relaxation grows linearly with the spontaneous polarization. The viscosities of the surface and bulk processes, as determined from measured characteristic times and spontaneous polarization, increase in a thermally activated manner for temperatures within the ferroelectric phase. Comparison of frequency-dependent optical response and dielectric response measurements at small applied fields shows that both are due to the same bulk molecular reorientation process.

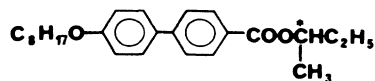
INTRODUCTION

Ferroelectric liquid crystals have been studied extensively in recent years due both to electro-optic effects which make them appear promising for optical display purposes, and their interesting basic chemical and physical properties.¹ The ferroelectricity occurs in tilted chiral smectic liquid crystals, which have layered structures with molecules tilted with respect to the layer planes. We recently completed a dielectric study of racemic and chiral forms of the commercially available liquid crystal CE8 (a British Drug House designation) which described in some detail the overall temperature dependences of the response of the two forms, as well as the characteristics of the low-frequency dielectric relaxation which was present only for the chiral $\text{Sm}C^*$ ferroelectric phase.² There have been many studies of the dielectric properties of DOBAMC [(*p*-decyloxybenzylidene)-*p*-amino-(2-methylbutyl) cinamate]. In this report we present the results of experiments in which the dielectric response of a smectic (Sm) liquid-crystal mixture which displays the $\text{Sm}C^*$ phase in the vicinity of room temperature was studied in detail. We also present results which correlate the dielectric relaxation in the $\text{Sm}C^*$ phase with the optical-switching behavior. In addition, the measurements, performed on a thin cell ($2.7 \mu\text{m}$), show the dramatic effects of dielectric relaxations due to reorientations at the cell surfaces.

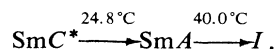
The material studied was 1:1 mixture $\text{C}_8\text{H}_{17}\text{COOC}_6\text{H}_4\text{O}_6\text{H}_4\text{COOCH}_2\text{CH}(\text{CH}_3)\text{C}_2\text{H}_5$ (BOH8),



and $\text{C}_8\text{H}_{17}\text{OC}_6\text{H}_4\text{C}_6\text{H}_4\text{COOCH}(\text{CH}_3)\text{C}_2\text{H}_5$ (MPOOBC)



The chirality, due to the methylbutyl units, allows for the occurrence of ferroelectricity. The chemistry of these materials has been described elsewhere.³ The sequence of phase transitions is



The dielectric measurements described here were all done in the $\text{Sm}C^*$ phase or in the $\text{Sm}A$ phase in the vicinity of the transition to $\text{Sm}C^*$.

Cells for the measurement of the dielectric response were made from indium tin oxide (ITO)-coated glass. The electrodes were $0.64 \times 0.64 \text{ cm}^2$ in area, and transparent to light. The cell thickness, $2.7 \mu\text{m}$, was maintained by a small number of spheres between the glass plates. Both inner surfaces of the cell were coated with approximately 300 Å of poly (1,4-butylene terephthalate), with one side buffed in a single direction. The buffing aligns the liquid-crystal molecules in the $\text{Sm}A$ phase. The smectic plane normals are assumed to be parallel to the plane of the electrodes for this geometry. Electric fields are applied parallel to the smectic layers. The BOH8/MPOOBC mixture was introduced into the cell at approximately 45°C , in the isotropic state. Electrical contact was made to the ITO with indium solder applied in a nitrogen-rich atmosphere.

Alignment of the molecules in the $\text{Sm}C^*$ phase was checked optically with the sample placed on a heating and/or cooling stage. In the ferroelectric $\text{Sm}C^*$ phase, the liquid-crystal orientation is bistable, with the spontaneous polarization pointing toward either of the glass plates. The tilt angle of the molecules is parallel to the plane of the plates. For this cell thickness, the pitch of the helix is suppressed due to surface forces and can therefore be thought of as being a very long (or infinite) value. The same stage was employed to determine the temperature dependence of the spontaneous polarization through measurement of the depolarization current released when the direction of the polarization was re-

versed with the application of a low-frequency sawtooth voltage waveform.⁴

The dielectric-constant measurements were made with the sample cell placed between the plates of a dc-powered thermoelectric module which allowed stable temperature variation in the vicinity of ambient temperature. Sample temperature was measured by a thermocouple attached to the outside of one glass plate just to the side of the electrode area. Temperature stability was better than 0.02 °C during the data-collection period (approximately 3 min) at each temperature. Relative temperature is known to 0.02 °C, but the absolute temperatures reported are probably good to only within 1 °C. Data were recorded on cooling. Because the phase transition is in the vicinity of ambient temperature, each data series was preceded by heating the sample into the isotropic phase to insure a self-consistent initial state. The real and imaginary parts of the sample conductivity (σ' and σ'') were measured between 5 Hz and 13 MHz at 20 frequencies per decade, employing a Hewlett-Packard HP4191A impedance analyzer under computer control. The measurement circuit was balanced such that stray conductances measured on a standard 1-k Ω test resistor in place of the sample were less than 3% of the true conductance.

The dielectric response was found to be dependent on the applied ac signal. Two sets of temperature-dependent data were collected: one, at 0.1 V rms ac level (370 V/cm) at 18 temperatures on cooling between 26.5 and 15.6 °C; and another, at 1.0 V rms ac level (3700 V/cm) at 19 temperatures on cooling between 25.4 and 13.85 °C. At one temperature, the signal-level dependence of the response was studied in detail within the above limits.

The frequency-dependent dielectric constants were obtained from the measured conductivities by $\epsilon'(\omega) = 4\pi\sigma(\omega)/\omega$ and $\epsilon''(\omega) = 4\pi[\sigma'(\omega) - \sigma_{dc}]/\omega$, where σ_{dc} is the conductivity at low frequencies where $\sigma'(\omega)$ was independent of ω . For some data sets, dispersion is observed in $\sigma'(\omega)$ even at the lowest frequency of the measurement, due to the presence of a dielectric relaxation at very low frequency. In those cases σ_{dc} was taken as zero. In order to best characterize the temperature dependence of the observed dielectric relaxations, the $\epsilon(\omega)$ data in the appropriate frequency range were fit to the semiempirical modification of the Debye response of a system with a single (Debye) relaxation time due to Havriliak and Negami,⁵

$$\epsilon(\omega) = \epsilon_{hf} + (\epsilon_0 - \epsilon_{hf}) / (1 + (1\omega\tau_0)^{1-\alpha})^\beta \quad (1)$$

Where $\epsilon(\omega)$ is the frequency-dependent dielectric response, τ_0 is the characteristic mean relaxation time, ϵ_0 is the static dielectric constant ($\omega \ll 1/\tau_0$) and ϵ_{hf} is the high frequency dielectric constant ($\omega \gg 1/\tau_0$). This generalization of the Debye formulation describes a system with a distribution of relaxation times associated with a single process, with the exponents α and β characterizing the width and skewness of the distribution of relaxation times about τ_0 , respectively. The response for a system with a single characteristic time is obtained for $\alpha=0$, $\beta=1$.

In the dielectric response of the BOH8/MPOBC mix-

ture at the 1-V signal level, *two* relaxations were observed. The second relaxation is due to molecular reorientation at the surface of the cell. In order to characterize the two relaxations, the data were fit to the sum of two distinct processes,

$$\epsilon(\omega) = \epsilon_{hf} + \frac{(\epsilon_0^{(1)} - \epsilon_0^{(2)})}{[1 + (i\omega\tau_0^{(1)})^{(1-\alpha^{(1)})}]^{\beta^{(1)}}} + \frac{(\epsilon_0^{(2)} - \epsilon_{hf})}{[1 + (i\omega\tau_0^{(2)})^{(1-\alpha^{(2)})}]^{\beta^{(2)}}}, \quad (2)$$

where ϵ_{hf} is the dielectric constant for $\tau \ll \tau_0^{(2)}$, and the parameters with superscript 1 describe the lower-frequency relaxation, whereas those with superscript 2 describe the higher-frequency relaxation. The fits to the data were made in all cases by minimization of the quantity

$$R = \sum_{\omega} \frac{[|\epsilon'_{obs}(\omega) - \epsilon'_{calc}(\omega)| + |\epsilon''_{obs}(\omega) - \epsilon''_{calc}(\omega)|]}{\sum_{\omega} [\epsilon'_{obs}(\omega) + \epsilon''_{obs}(\omega)]}, \quad (3)$$

where the sum is taken for all available $\epsilon(\omega)$ points.

The optical equivalent of the frequency-dependent dielectric measurement was performed at one temperature to establish the relationship between the dielectric relaxation and optical switching in the ferroelectric phase. The sample was placed in the cooling stage between crossed polarizers at a temperature within the SmC* region. A beam of light was transmitted through the sample and polarizer and detected by a fast, light-sensitive diode detector. A sinusoidal voltage was applied to the sample, and the current emitted by the light-sensitive diode amplified by a Keithley 417 current amplifier. The liquid-crystal cell was oriented such that the maximum contrast at very low frequencies (difference between minimum and maximum detector current) was obtained. The difference in detector current comes from the modulation of the constant-intensity light source by the switching of the direction of the polarization of the liquid crystal by the electric field, which causes a change in the orientation of the long axis of the molecules within the plane of the cell. (This molecular reorientation is the basis for the use of smectic liquid crystals for optical displays.) In direct analogy to the dielectric measurements, the detector current and voltage applied to the liquid-crystal display are in phase at low frequencies where the molecules can easily follow the electric field, and become out of phase as the molecules cannot respond quickly enough to the field at high frequencies. Thus a measurement of in-phase and out-of-phase components of the contrast through the measurement of the in-phase and out-of-phase detector current (lock-in amplifier) yields the frequency-dependent characterization of the molecular process which governs the optical switching. The optical-switching measurements were made at frequencies between 10 and 10⁴ Hz at applied voltages between 0.025 and 0.1 V rms. For voltages in excess of approximately 0.5 V rms the current waveform in response to a sinusoidal applied-voltage waveform was no longer sinusoidal, as the contrast sa-

tured to a constant value for instantaneous values of the applied voltage greater in magnitude than approximately 0.5 V.

RESULTS

The dielectric response within the SmC^* phase for the $2.7\mu\text{m}$ cell at applied ac voltages between 0.01 and 0.30 V rms was found to be independent of the test-signal level. An applied signal of 0.1 V rms was therefore chosen to characterize the small signal response as a function of temperature. The frequency-dependent dielectric measurements show the dramatic appearance and growth of a low-frequency dielectric relaxation on entering the SmC^* phase from the SmA phase. The characteristic time for the relaxation shows a dramatic increase as the SmC^* to SmA transition is approached from above and below. Examples of the frequency-dependent dielectric data for the small signal response are presented in Fig. 1 for a range of temperature of 0.35°C in the vicinity of the phase transition. Two "relaxations" are observed in the frequency range of the measurement. The relaxation at frequencies near 10^6 Hz is actually due to the series RC circuit which arises from the capacitance of the parallel-plate electrodes in series with the tin ITO contacts and the indium-ITO contact resistance. This relaxation is present in cells of this geometry without the presence of liquid crystals² and can be shifted to higher frequencies by the application of thicker Ta or Cr (not transparent) electrodes. The low-frequency relaxation increases in strength and decreases in frequency as the SmC^* phase is entered on cooling. To characterize the relaxation, the dielectric data for $\epsilon'(\omega)$ and $\epsilon''(\omega)$ were fit to Eq. (2). This involved between 212 and 154 $\epsilon'(\omega)$ and $\epsilon''(\omega)$ points, dependent on temperature. The smaller number of points is fit at high tempera-

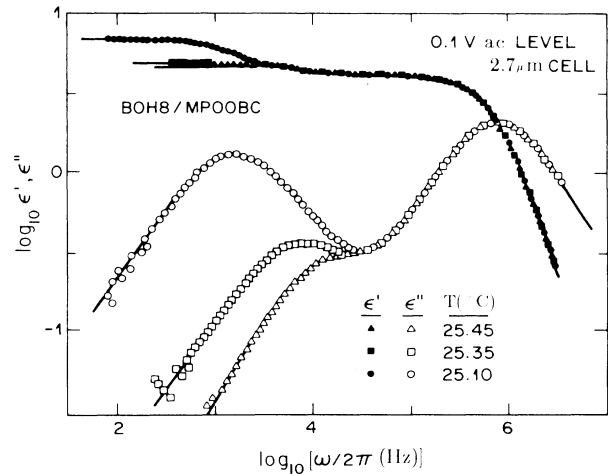


FIG. 1. Logarithm of the real (ϵ' , solid symbols) and imaginary (ϵ'' , open symbols) parts of the dielectric response vs logarithm of frequency for three selected temperatures, 0.1-V ac signal level. Solid lines from fits of the data to Eq. (2).

tures as the minimum frequency is taken as the point where $\sigma'(\omega) - \sigma_{\text{dc}}$ deviates from zero, which occurs at higher frequencies when the low-frequency relaxation occurs at higher frequencies. The circuit relaxation is independent of temperature, as expected, with a Debye character ($\alpha^{(2)}=0, \beta^{(2)}=1$) and a characteristic time $\tau_0^{(2)}=2.0 \times 10^{-7}$ sec. At low temperatures (e.g., 25.10°C , Fig. 1) inclusion of the circuit relaxation in the fit is not important as the two processes occur at considerably different frequencies. Its inclusion at higher temperatures, however, allows us to determine the characteristics of the

TABLE I. Parameters describing the dielectric response of BOH8/MPOOBC in the linear-response regime (0.1-V applied signal) by fits to Eq. (1). $\epsilon_{\text{hf}}=4.10$, fitted.

T ($^\circ\text{C}$)	ϵ_0	α	β^a	τ_0 (sec)	$\omega_0/2\pi$ (Hz)	R (%) ^b
26.5	4.20	0	1	5.0×10^{-6}	3.2×10^4	0.6
26.2	4.24	0	1	5.0×10^{-6}	3.2×10^4	0.8
26.1	4.24	0	1	7.0×10^{-6}	2.3×10^4	0.6
25.9	4.30	0	1	8.0×10^{-6}	2.0×10^4	0.6
25.75	4.36	0	1	7.0×10^{-6}	2.3×10^4	1.0
25.47	4.52	0	1	1.2×10^{-5}	1.3×10^4	1.0
25.35	4.82	0.10	1.11	2.0×10^{-5}	8.0×10^3	0.7
25.10	6.84	0.10	1.11	9.0×10^{-5}	1.8×10^3	1.4
25.07	9.96	0.27	1.37	1.8×10^{-4}	8.8×10^2	1.8
24.97	16.28	0.24	1.32	3.9×10^{-4}	4.1×10^2	1.9
24.90	18.23	0.29	1.41	5.0×10^{-4}	3.2×10^2	2.1
24.67	16.60	0.27	1.37	4.8×10^{-4}	3.3×10^2	2.0
23.47	11.39	0.10	1.11	3.8×10^{-4}	4.2×10^2	1.8
22.27	10.42	0.10	1.11	3.5×10^{-4}	4.6×10^2	1.3
20.52	10.42	0.10	1.11	3.5×10^{-4}	4.6×10^2	1.4
18.65	10.42	0.10	1.11	3.8×10^{-4}	4.2×10^2	1.6
17.17	10.42	0.10	1.11	4.0×10^{-4}	4.0×10^2	1.7
15.60	10.42	0.13	1.11	4.2×10^{-4}	3.8×10^2	1.9

^a $\beta=1/(1-\alpha)$, not fitted.

^b R is the agreement index, Eq. (3).

liquid-crystal response in an interesting temperature range. In the fits to Eq. (2) the circuit characteristics $\tau_0^{(2)}$, $\alpha^{(2)}$ and $\beta^{(2)}$ were determined at low temperatures and then not varied in the determination of the liquid-crystal relaxation parameters. The data were fit with the four parameters $\epsilon_0^{(1)}$ ($=\epsilon_0$), $\epsilon_{hf}^{(2)}$ ($=\epsilon_{hf}$), $\tau_0^{(1)}$ ($=\tau_0$) and $\alpha^{(1)}$ ($=\alpha$). It was found that $\beta(1-\alpha)=1$ for all temperatures and it was therefore constrained by that relationship in the refinement of α . The dielectric data are fit to an excellent approximation by Eq. (2), which has reduced to the form of Eq. (1) in the refinement, with the average agreements between the observed and calculated $\epsilon(\omega)$ points between 0.6% and 2.1%. The results are presented in Table I, in terms of the parameters of Eq. (1). Approximate relative errors are 0.02 for ϵ_0 and ϵ_{hf} , 0.03 for α , 3% for τ_0 at low temperatures, and 10% for τ_0 at the highest temperatures (where the relaxation time of the liquid crystal is close to that of the circuit). The characteristic frequency of the relaxation ($\omega_0=1/\tau_0$) is also presented in the table. The solid lines in Fig. 1 are from the fits to the data.

The characteristic time of the dielectric relaxation for the BOH8/MPOOBC mixture increases by approximately 2 orders of magnitude in the 11°C range of the measurements. The temperature dependence of τ_0 is presented in Fig. 2 on a linear scale. The relaxation is present, with a fast relaxation time, at temperatures 1–2°C above the SmA to SmC* transition, and slows down dramatically in the approximately 0.5°C temperature interval just before the transition which is at the peak in τ_0 . This critical-like slowing down, by about 2 orders of magnitude in time, is more dramatic than that observed previously at SmA to SmC* transitions in liquid crystals, e.g., DOBAMC (Ref. 6), where the relaxation time also slows down as T approaches T_c from below, but only by 30%. For temperatures more than approximately 4°C below the transition, the relaxation time is decreasing with decreasing temperature in a manner consistent with a thermally activated process. The frequency of the relaxation for temperatures away from T_c within the SmC* phase (400–500 Hz) is similar to those reported for other ferroelectric liquid

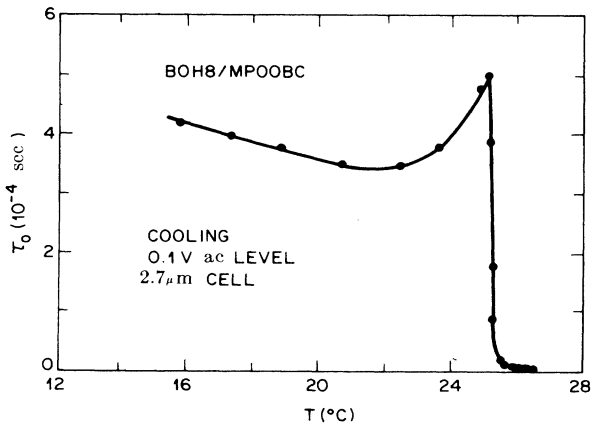


FIG. 2. Temperature dependence of the characteristic time of the dielectric relaxation (Table I) at the 0.1-V ac signal level.

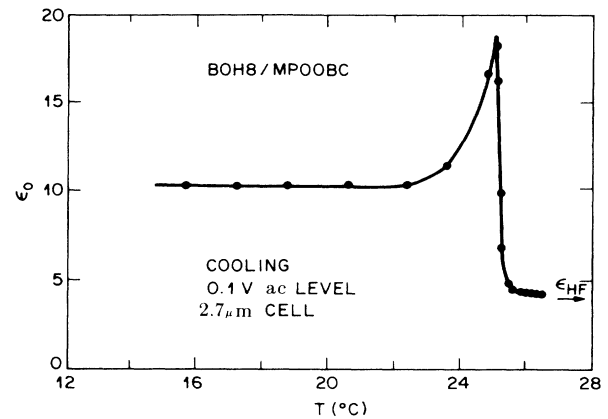


FIG. 3. Temperature dependence of the static dielectric constant (Table I) at the 0.1-V ac signal level

crystals such as DOBAMC (Ref. 6) but slower than that we found for CE8 (~ 1500 Hz) in its ferroelectric phase.²

The dielectric constant for frequencies much larger than the characteristic frequency of the relaxation, $\epsilon_{hf}=4.10$, is independent of temperature in the range studied. The low-frequency dielectric constant ϵ_0 , characterizing the dielectric strength of the ferroelectric relaxation, shows dramatic changes in the dielectric permittivity of the liquid crystal in the vicinity of the SmA to SmC* transition. The temperature dependence of ϵ_0 for the 0.1-V applied ac signal is presented in Fig. 3. Within a temperature range of 1°C of the phase transition, ϵ_0 rises to a maximum of 18.2 after which it decreases to a value of 10.4 which is independent of temperature at temperatures more than 4°C below the phase transition. Thus ϵ_0 shows critical-type behavior as T_c is approached from above and below. In conjunction with the slowing down of the relaxation time in the same temperature interval, these data are the clearest example of this kind of behavior in ferroelectric liquid crystals to date. The temperature dependence of ϵ_0 , especially, is considerably different than that usually observed, which is similar to our higher-signal data. The distribution of relaxation times, described by the parameters α and β , shows interesting behavior. On cooling in the SmA phase, the relaxation is *not* distributed, but Debye-like. In the vicinity of the phase transition, the distribution broadens considerably, then narrows again at lower temperatures. The distribution of relaxations, where not Debye-like, is somewhat asymmetric.

The dielectric response of BOH8/MPOOBC mixture is quite different at the 1.0-V ac signal level (3700 V/cm) than the 0.1-V signal level (370 V/cm). An example of the effect of signal level on the response is shown in Fig. 4, illustrating only the frequency regime of the liquid-crystal response, at a temperature of 15.75°C. The response shown at $V_{ac}=0.25$ V rms is identical to those at lower voltages. At this temperature, within the SmC* phase, at signals greater than approximately 0.3 V/cm, the appearance of a second, very-low-frequency relaxation is observed whose characteristic frequency increases with increasing signal level. By a signal level of 1 V rms the

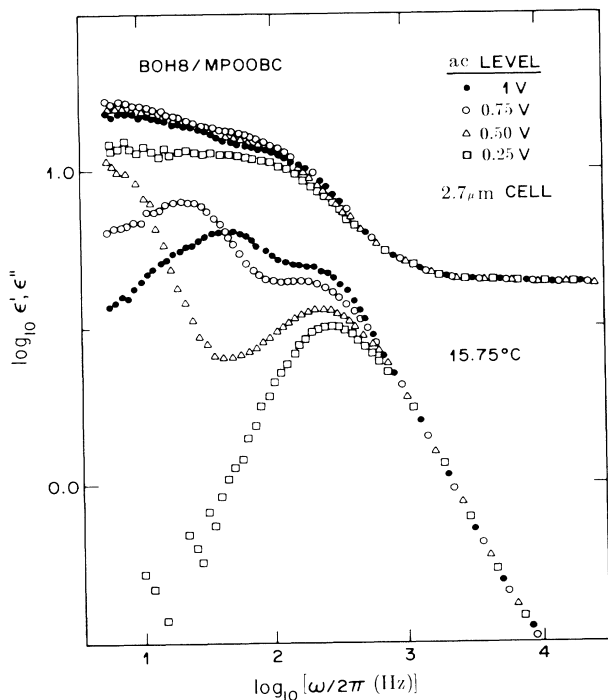


FIG. 4. Logarithm of the real and imaginary parts of the dielectric response in the frequency range of the liquid-crystal dielectric relaxation as a function of applied ac voltage. The response is independent of applied signal for voltages less than 0.3 V rms.

frequency of the second relaxation is well within the frequency range of our measurement technique, allowing us to analyze both relaxations in detail as a function of temperature.

At the 1-V signal level, the response of the liquid crystal to the applied field is nonlinear in nature. This manifests itself in the fact that the imaginary part of the dielectric response $\epsilon''(\omega)$, derived from $\sigma'(\omega) - \sigma_{dc}$, can no longer be fit well by equations like Eq. (1). An example of the discrepancy in fitting $\epsilon'(\omega)$ and $\epsilon''(\omega)$ is presented in Fig. 5. The $\epsilon'(\omega)$ data have been fit to a single relaxation at 3.6 kHz (the second relaxation appears at lower temperatures) with a distribution of relaxation times described by $\alpha=0.23$, $\beta(1-\alpha)=1$. The fit to $\epsilon'(\omega)$ is excellent, with an average agreement of 0.6% between observed and calculated values. The discrepancy for $\epsilon''(\omega)$ is clearly seen by comparison of the observed data (open circles) to the line calculated for $\epsilon''(\omega)$ from the fit to $\epsilon'(\omega)$. For all temperatures, $\epsilon''(\omega)$ observed is larger than that calculated from fits to $\epsilon'(\omega)$, with the discrepancy increasing with decreasing temperature. The $\epsilon''(\omega)$ data, if attributed to the dielectric relaxation, are physically unreasonable, as evidenced by two observations: (1) even at temperatures where the $\epsilon'(\omega)$ data are described by a Debye response ($\alpha=0, \beta=1$), $\epsilon''(\omega)$ is larger than the calculated values, a situation which is in violation of the Kramers-Kronig relationship, and which cannot therefore be described by any formalism for dielectric relaxation and (2) the slope of

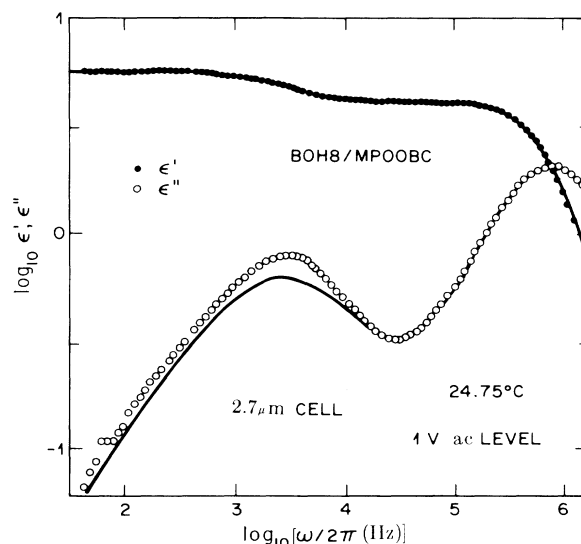


FIG. 5. Logarithm of the real (solid circles) and imaginary (open circles) parts of the dielectric response vs the logarithm of frequency for the 1-V ac signal level at 24.75°C. Solid line is from the fits to Eq. (2), illustrating the agreement for ϵ' and disagreement for ϵ'' .

$\epsilon''(\omega)$ versus $\log \omega$ for frequencies larger than ω_0 is greater than -1 , a physical impossibility; in this case (Fig. 5), for instance $\beta(1-\alpha)=1.3$ fits the $\epsilon''(\omega)$ data for $\omega > \omega_0$. There are two possible explanations for $\epsilon''(\omega)$ data which are inconsistent with $\epsilon'(\omega)$ data for a dielectric relaxation as we have observed: (1) There is an additional physical processes operating at low frequencies which results in a frequency-dependent real conductivity. One possibility for such a process is a distributed ionic conductivity as has been observed in some ionic conductors⁷ and liquid crystals⁸. (2) The frequency-response analyzer measures the in-phase component of the conductivity $\sigma'(\omega)$ in response to the applied signal erroneously. We have observed the current waveform in the SmC* phase at low frequencies for an applied signal of 1.0 V rms. The response to the sinusoidal voltage signal is a slightly distorted current signal. The distortion occurs for instantaneous voltages near the maximum deviation from 0, greater than ± 1 V, where the current waveform becomes asymmetric. The asymmetry is due to the fact that cell has been buffed on one side (to align the liquid crystal) and not on the other, and though a very minor asymmetry at 1.0-V ac levels, becomes pronounced for signals larger than 3.5 V rms. Although the current waveform distortion is not large at the 1.0-V ac level, its presence makes it difficult for us to distinguish which of the two possibilities is giving rise to the observed $\epsilon''(\omega)$ data. The minor nature of the waveform distortion suggests to us, however, that (1) may well be the case.

Considering the above, and the fact that the $\epsilon'(\omega)$ data are very well behaved, we have fit the observed $\epsilon'(\omega)$ data at the 1-V signal level to Eq. (2) in the temperature range 25.4°C to 13.85°C. The fitting parameters describing the dielectric response of BOH8/MPOOBC at 1-V signal lev-

TABLE II. Parameters describing the dielectric response of BOH8/MPOOBC in the nonlinear-response regime (1-V applied signal) by fits to Eq. (2).

T (°C)	$\epsilon_0^{(1)}$	$\epsilon_0^{(2)}$	ϵ_{hf}	$\alpha^{(1)}$	$\beta^{(1)a}$	$\alpha^{(2)}$	$\beta^{(2)b}$	$\tau_0^{(1)}$ (sec)	$\omega_0/2\pi^{(1)}$ (Hz)	$\tau_0^{(2)}$ (sec)	$\omega_0/2\pi^{(2)}$ (Hz)	$R(\%)^b$
25.40	4.49		4.17	0.17	1.20			6.0×10^{-6}	2.7×10^4			0.4
25.30	4.62		4.17	0.23	1.30			8.0×10^{-6}	2.0×10^4			0.2
25.20	4.75		4.17	0.23	1.30			1.0×10^{-5}	1.6×10^4			0.4
24.95	5.34		4.17	0.23	1.30			2.7×10^{-5}	5.9×10^3			0.4
24.75	5.86		4.17	0.23	1.30			4.4×10^{-5}	3.6×10^3			0.6
24.65	6.71		4.17	0.15	1.18			9.5×10^{-5}	1.7×10^3			0.6
24.40	7.81		4.17	0	1			2.6×10^{-4}	6.1×10^2			1.1
24.30	9.11	4.36	4.20	0	1	0	1	4.2×10^{-4}	3.8×10^2	6.0×10^{-5}	2.7×10^3	1.1
24.10	9.11	4.49	4.20	0	1	0	1	4.3×10^{-4}	3.7×10^2	6.7×10^{-5}	2.4×10^3	1.1
24.00	9.43	4.69	4.20	0	1	0	1	4.8×10^{-4}	3.3×10^2	7.3×10^{-5}	2.2×10^3	1.1
23.75	10.22	5.01	4.20	0	1	0	1	6.0×10^{-4}	2.7×10^2	1.0×10^{-4}	1.6×10^3	1.0
23.40	10.54	5.53	4.20	0	1	0	1	6.9×10^{-4}	2.3×10^2	1.5×10^{-4}	1.1×10^3	1.0
22.85	11.07	6.51	4.20	0	1	0	1	9.0×10^{-4}	1.8×10^2	1.8×10^{-4}	8.8×10^2	1.0
21.95	12.04	7.81	4.20	0	1	0	1	1.3×10^{-3}	1.2×10^2	2.5×10^{-4}	6.4×10^2	0.9
20.65	13.02	9.11	4.20	0	1	0	1	2.1×10^{-3}	7.5×10^{-4}	3.0×10^{-4}	5.3×10^2	1.0
19.20	13.67	10.42	4.20	0	1	0	1	3.0×10^{-3}	5.3×10^{-4}	3.5×10^{-4}	4.5×10^2	1.0
17.35	14.32	11.39	4.20	0	1	0	1	4.8×10^{-3}	3.3×10^1	4.4×10^{-4}	3.6×10^2	1.0
16.05	14.65	12.04	4.20	0	1	0	1	8.4×10^{-3}	1.9×10^1	5.2×10^{-4}	3.1×10^2	1.0
13.85	14.65	12.69	4.20	0	1	0	1	1.2×10^{-2}	1.3×10^1	6.3×10^{-4}	2.5×10^2	1.4

^a $\beta = 1/(1-\alpha)$ not fitted.

^b R is the agreement index, Eq. (3), $\epsilon^1(\omega)$ data only.

el are presented in Table II. The parameters with superscript (1) describe the low-frequency relaxation, and those with superscript (2) describe the high-frequency relaxation. As described by Eq. (2), the strength of the low-frequency relaxation is given by $(\epsilon_0^{(1)} - \epsilon_0^{(2)})$ and that of the high-frequency relaxation by $(\epsilon_0^{(2)} - \epsilon_{hf})$. The frequency range of the circuit response (above 10^4 Hz) has been omitted from the fits. The fits include between 55 and 65 $\epsilon'(\omega)$ points. For temperatures of 24.40°C or greater, the data have been fit by four parameters, $\epsilon_0^{(1)}$, ϵ_{HF} , $\alpha^{(1)}$, and $\tau_0^{(1)}$, [$\beta(1-\alpha)=1$] as the second relaxation appears only at low temperatures. At temperatures below 24.40°C the data have been fit by five parameters, $\epsilon_0^{(1)}$, $\epsilon_0^{(2)}$, ϵ_{hf} , $\tau_0^{(1)}$, and $\tau_0^{(2)}$. As seen in the table, we found $\alpha^{(1)} = \alpha^{(2)} = 0$, $\beta^{(1)} = \beta^{(2)} = 1$, at low temperatures, pure Debye responses, and have fixed those parameters in the fits. The data have been fit to an excellent approximation by Eq. (2), with average agreements generally near 1%. Estimations of the errors in the parameters are 0.02 for $\epsilon_0^{(1)}$, $\epsilon_0^{(2)}$, and ϵ_{hf} , ± 0.03 for $\alpha^{(1)}$ and $\pm 3\%$ for $\tau_0^{(1)}$ and $\tau_0^{(2)}$. The characteristic frequencies of the relaxation are also presented in the table. Examples of the $\epsilon'(\omega)$ data at four representative temperatures are presented in Fig. 6. The solid lines, drawn from the parameters in Table II, show the excellent fit of the model to the data. The $\epsilon'(\omega)$ data in Fig. 6 have been selected to illustrate the appearance of the high-frequency relaxation at 24.3°C and its increasing strength with decreasing temperature. Also apparent in the figure is the decrease in the characteristic frequencies of both relaxations with decreasing temperature.

The characteristic time of the low-frequency dielectric relaxation in the BOH8/MPOOBC mixture at 1-V ac level changes by more than 4 orders of magnitude in the

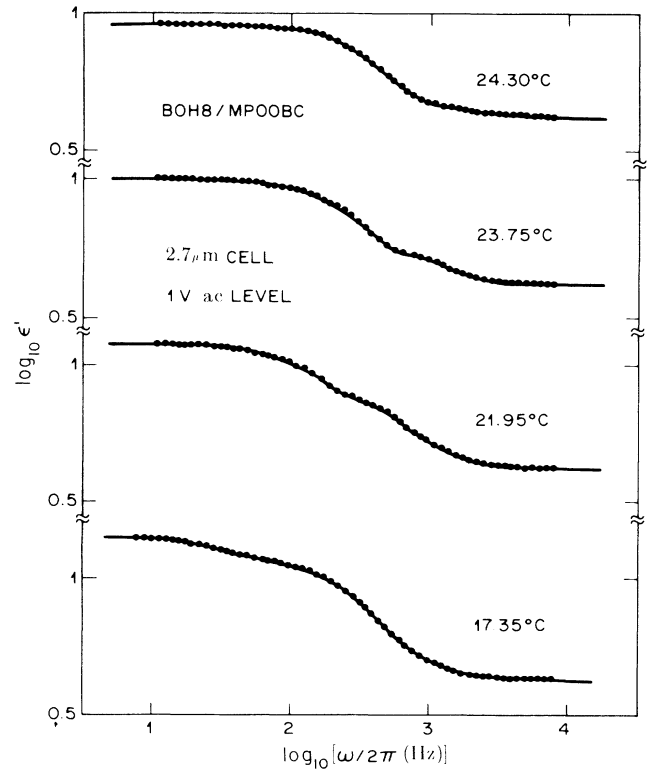


FIG. 6. Logarithm of the real part of the dielectric response vs logarithm of frequency at the 1-V signal level as a function of temperature. The growth of the high-frequency relaxation with decreasing temperature is illustrated. The solid lines are from the fits to Eq. (2). Vertical axes displaced for clarity.

11.5°C temperature interval of the experiment. A dramatic rise of more than 2 orders of magnitude occurs in the SmA phase within 1°C of the transition to the SmC* phase. The second relaxation, at higher frequency, appears when the liquid crystal enters the SmC* phase. The characteristic times for both relaxations as a function of temperature are presented in Fig. 7. When the high-frequency relaxation appears, its characteristic frequency is relatively high (2700 Hz) but within 4°C of the phase transition this decreases to less unusual values of a few hundred Hz. For the low-frequency relaxation, the frequencies are actually very high in the SmA phase (as high as 27 kHz) but decrease to very low frequencies (13 Hz) by 10°C below the phase transition. This low-frequency relaxation, described by $\tau_0^{(1)}$, is the one which appeared with increasing ac level described in reference to Fig. 4. Its characteristic frequency is dramatically dependent on temperature and ac signal level. The high-frequency relaxation described by $\tau_0^{(2)}$ at the 1-V signal level is the same relaxation present in the 0.1-V signal-level data (Fig. 4). The characteristics of this relaxation are also signal dependent, as can be seen by comparison of Figs. 7 and 2, especially with regard to the critical-like showing down of the relaxation in the vicinity of T_c observed in the small-signal data, not observed in the large-signal data.

The peak in the dielectric permittivity in the vicinity of the SmA to SmC* phase transition is also not observed for the large-signal data. The temperature dependencies of $\epsilon_0^{(1)}$ and $\epsilon_0^{(2)}$ are presented in Fig. 8. The strength of the low-frequency relaxation ($\epsilon_0^{(1)} - \epsilon_0^{(2)}$) increases in the SmA phase as it slows down on approaching the phase transition. The high-frequency relaxation first appears at the phase transition and grows slowly in strength ($\epsilon_0^{(2)} - \epsilon_{HF}$) as temperature decreases. The forms of these curves are more similar to those usually observed for liquid crystals^{6,9,10} in contrast to that in Fig. 3. At temperatures more than a few degrees below the phase transition, the growth of the low-frequency relaxation has slowed considerably, and the high-frequency relaxation is dominating

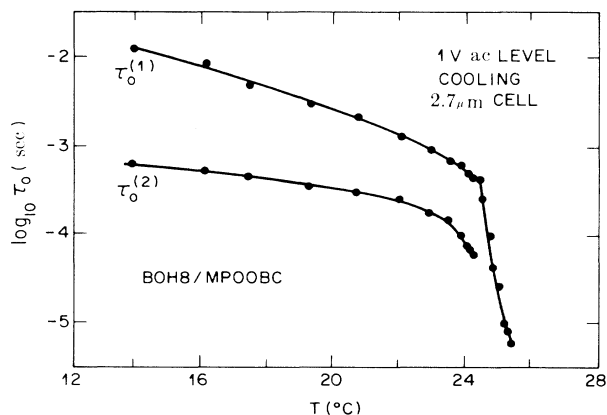


FIG. 7. Logarithm of the characteristic times of the low ($\tau_0^{(1)}$) and high ($\tau_0^{(2)}$)-frequency dielectric relaxations as a function of temperature (1-V ac signal level, Table II).

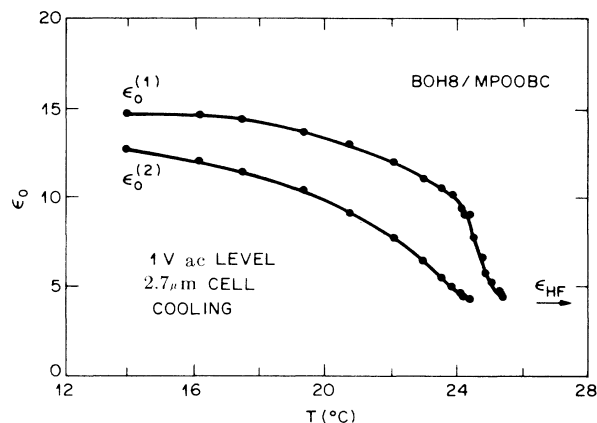


FIG. 8. Temperature dependence of the very-low-frequency dielectric constant $\epsilon_0^{(1)}$ and intermediate-frequency dielectric constant $\epsilon_0^{(2)}$ [see Eq. (2)] at the 1-V signal level (Table II).

the dielectric response of the liquid crystal. By about 10°C below the phase transition the high-frequency relaxation accounts for 80% of the total enhanced dielectric constant in the ferroelectric phase. The growth of the strength of high-frequency response ($\epsilon_0^{(2)} - \epsilon_{HF}$) with decreasing temperature relative to the total response ($\epsilon_0^{(1)} - \epsilon_{HF}$) is presented in Fig. 9. The low-frequency relaxation in the SmA phase shows a small distribution of relaxation times ($\alpha \sim 0.2$), whereas on entering the SmC* phase the relaxations at both low and high frequencies have single relaxation times with no distribution ($\alpha = 0$).

Characterization of the behavior of the liquid crystal in further detail can be made if the spontaneous polarization in the ferroelectric SmC* phase is known. The spontaneous polarization was measured for the BOH8/MPOOBC mixture as a function of temperature by the techniques

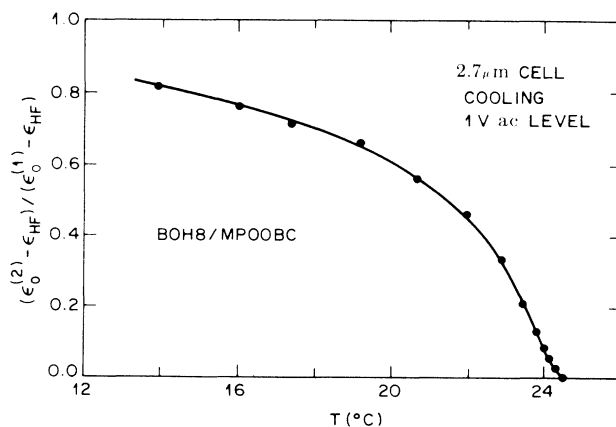


FIG. 9. Ratio of the dielectric strength of the high-frequency relaxation ($\epsilon_0^{(2)} - \epsilon_{HF}$) to the total enhancement of the dielectric constant in the ferroelectric phase ($\epsilon_0^{(1)} - \epsilon_{HF}$) vs temperature.

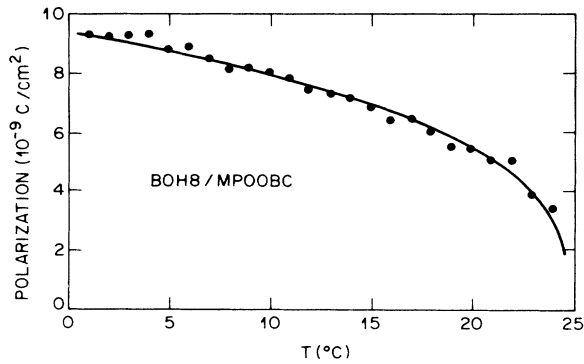


FIG. 10. Temperature dependence of the spontaneous polarization. Solid line is from the fit to Eq. (4).

described earlier and is presented in Fig. 10. The temperature dependence of the spontaneous polarization is described well by the expression

$$P_s(T) = P_0(T_c - T)^n, \quad (4)$$

where $P_0 = 3.25$, $T_c = 24.8^\circ\text{C}$, and $n = 0.324$, plotted as the solid line in Fig. 10. (We do not consider the 0.4°C difference between the measurement of T_c in the two different apparatuses to be significant.) The magnitude of the spontaneous polarization observed for this sample is similar to those commonly observed for other ferroelectric liquid crystals.

With the knowledge of the temperature dependence of P_s , the origin of the temperature dependence of the strength of the high-frequency dielectric relaxation can be determined. In Fig. 11, the dielectric strengths (1-V ac signal) of the low-frequency ($\epsilon_0^{(1)} - \epsilon_0^{(2)}$) and high-frequency ($\epsilon_0^{(2)} - \epsilon_{\text{HF}}$) relaxations are plotted versus P_s . The strength of the high-frequency relaxation grows linearly with P_s , indicating that this relaxation is due to the bulk relaxation of the electric dipoles. This is the re-

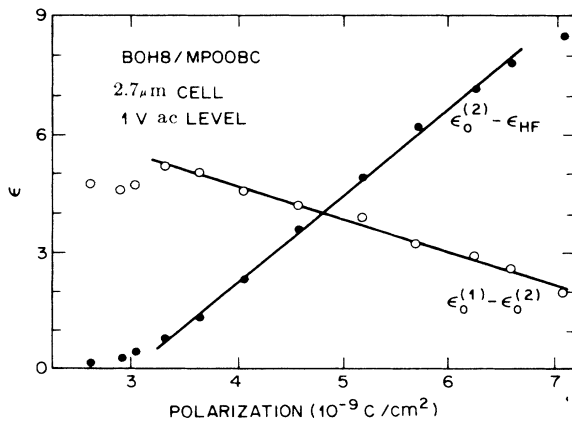


FIG. 11. Dielectric strengths of the high-frequency relaxation ($\epsilon_0^{(2)} - \epsilon_{\text{HF}}$) and the low-frequency relaxation ($\epsilon_0^{(1)} - \epsilon_0^{(2)}$) vs spontaneous polarization in the ferroelectric phase.

laxation which is present in the small-signal data, and so the critical behavior observed for ϵ_0 and τ_0 in that case is related to bulk molecular reorientation processes. Also shown in the figure is that the strength of the low-frequency relaxation decreases linearly with increasing P_s . The dramatic temperature and applied signal-level dependencies of the characteristics of this relaxation indicate that it is due to the occurrence of molecular reorientation at the surfaces of the cell. The molecular reorientations at the surfaces occur through the motion of domain walls. As the number of domain walls is not changing with temperature, the data indicate that the permittivity of the motion involving domain walls decreases with decreasing temperature, apparently linearly as the bulk polarization increases.

The rapid increase in the characteristic times of the bulk and surface relaxations with decreasing temperature suggests that the relaxation processes are thermally activated. In Fig. 12 we present the dependence of the logarithms of the characteristic times $\tau_0^{(1)}$ and $\tau_0^{(2)}$ versus $1000/T$, a representation which results in straight lines if $\tau_0 \propto \exp(-\delta/T)$. The characteristic times increase rapidly in the vicinity of the phase transition, but then follow an activated type behavior for temperatures within the ferroelectric phase. The activation energy for the surface relaxation process ($\tau_0^{(1)}$) is approximately twice that of the bulk process. The temperature dependence of the characteristic relaxation times is not expected to be strictly Arrhenius in behavior, however, as the spontaneous polarization is also temperature dependent. The characteristic relaxation time is expected to be dependent on the electric field (E) spontaneous polarization $P(T)$ and liquid-crystal viscosity $\eta(T)$ by the relationship¹¹

$$\frac{1}{\tau(T)} = \frac{P_s(T)E}{\eta(T)} \quad (5)$$

with true Arrhenius behavior expected for the viscosity $\eta(T)$. The liquid-crystal viscosities for the surface ($\eta^{(1)}$) and bulk ($\eta^{(2)}$) molecular reorientation processes as deter-

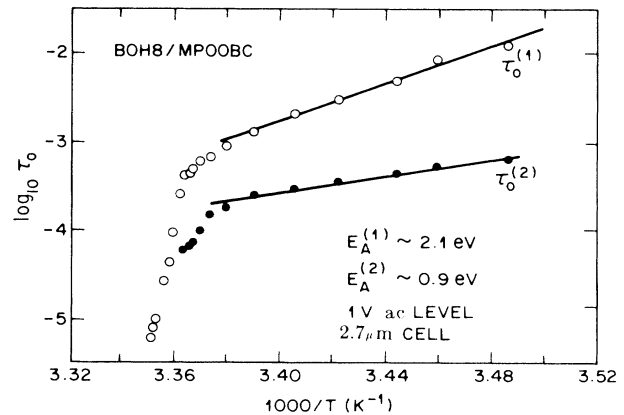


FIG. 12. Logarithm of the characteristic times of the low-frequency relaxation ($\tau_0^{(1)}$, open symbols) and the high-frequency relaxation ($\tau_0^{(2)}$, solid symbols) plotted vs $1000/T$.

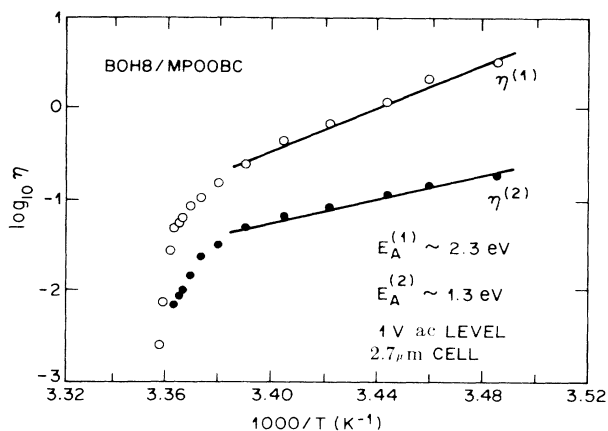


FIG. 13. Logarithm of the viscosity $\eta(T)$, determined from measured $P(T)$ and $\tau_0(T)$ and Eq. (5), vs $1000/T$ in the ferroelectric phase.

mined from measured values of $\tau_0^{(1)}$, $\tau_0^{(2)}$, and P_s are presented in Fig. 13. The viscosities of the processes increase with decreasing temperature, and a few degrees into the ferroelectric phase display an activated temperature dependence. The activation energy for the surface reorientation viscosity, 2.3 eV, is large, somewhat less than twice that of the viscosity for the bulk reorientation processes, 1.3 eV. The surface viscosity $\eta^{(1)}$ is larger than the bulk viscosity $\eta^{(2)}$ for all temperatures, with the difference increasing with decreasing temperature. The viscosity of the bulk molecular reorientation process is on the order of 10^{-1} P whereas that for the surface reorientation process is on the order of 1 P.

In the final series of experiments, the equivalence of the dielectric relaxation and the optical-switching processes was established. The experiments involved the measurement of the in-phase and out-of-phase components of the light contrast, C' and C'' , on measuring the light transmission through the liquid-crystal cell when switched with a sinusoidal voltage, by the technique described earlier. The results at 19°C are presented in Fig. 14 for three different ac signal levels. It is immediately apparent that the optical-switching response mirrors the behavior of the dielectric response very closely. The in-phase component C' saturates to a constant value at low frequencies, with a very small out-of-phase component C'' . As frequency is increased C' decreases and the phase difference between the contrast and the applied signal increases until the characteristic time for the molecular switching is reached and C' reaches a maximum. The optical switching is found to be a Debye-like process at 19°C as can be seen in the fact that $C''_{\text{max}} = 1/2 C'_{\text{max}}$. The data at three signal levels, when compared, indicate that at these levels the response of the optically switching liquid crystal is in the linear regime: (1) the in-phase component of the contrast at low frequencies where the molecules follow the field is linearly dependent on signal level, indicating a constant "permittivity" and (2) the characteristic frequency of the

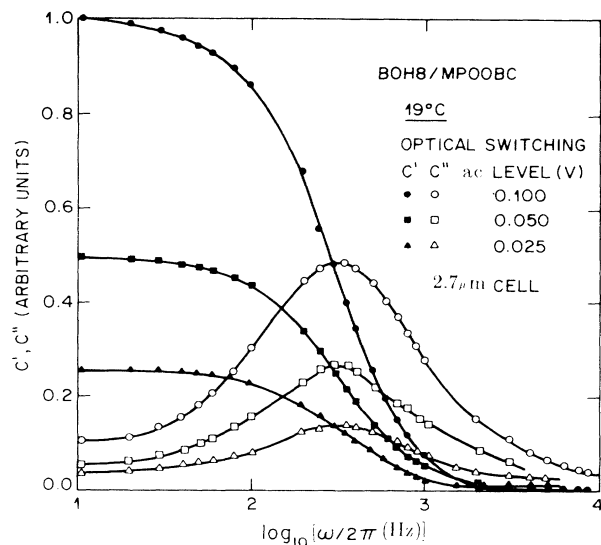


FIG. 14. Optical switching of the liquid-crystal cell at 19°C for small ac signal levels. Solid symbols, in-phase components of the contrast (c'); open symbols, out-of-phase components of the contrast (c'').

optical switching is independent of the applied field. Both of these results were also established in the dielectric-response measurements, where the dielectric response was found to be independent of applied electric field for signals up to 0.3 V rms.

Finally, we present in Fig. 15 a comparison of the dielectric-relaxation and optical-contrast data at approximately the same temperature. The comparison shows that the characteristic times of the two processes are identical,

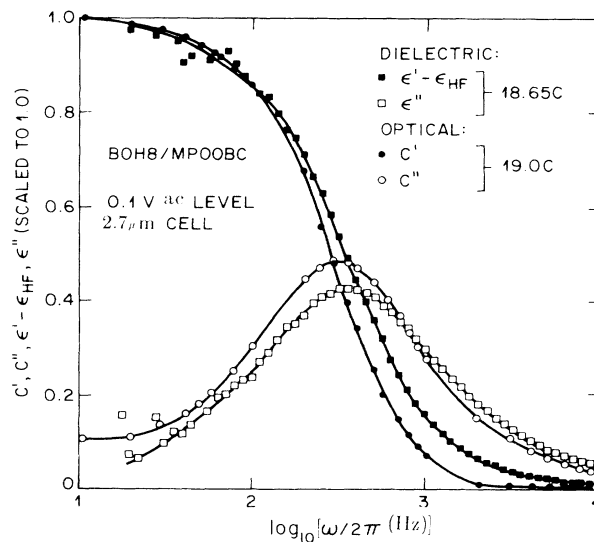


FIG. 15. Comparison of the in-phase and out-of-phase components of the dielectric response (ϵ' and ϵ'') with the in-phase and out-of-phase components of the optical contrast response (c' and c'') at approximately the same temperatures. Solid symbols, in-phase response; open symbols, out-of-phase response.

within experimental error, and that therefore the dielectric relaxation and optical switching are both due to the same molecular process. That molecular process we have shown in the dielectric measurements to be the relaxation of the molecular dipoles in the bulk of liquid crystal. The difference in the relative heights of the ϵ'' and C'' peaks reflect the fact that the optical switching is Debye-like [$\alpha=0, \beta(1-\alpha)=1$] whereas the dielectric relaxation has a small but significant distribution of characteristic times [$\alpha=0.1, \beta(1-\alpha)=1$]. We do not know the reason for this difference at the present time.

CONCLUSIONS

The experiments we have performed on the BOH8/MPOBC liquid-crystal mixture in and near its SmC^* phase indicate several interesting aspects of ferroelectric liquid-crystal behavior in thin cells. At low ac probe field levels a dielectric relaxation appears on approaching the SmC^* phase from the SmA phase. The characteristic time and dielectric permittivity of this relaxation display critical-like behavior near the phase transition. The dielectric response is independent of ac field strength in this regime. The molecular process which gives rise to the relaxation is the same molecular process which determines the optical-switching behavior. We have shown this process to be molecular reorientation in the bulk of the sample. As there are no disclinations in this sample, no ambiguity exists in the assignment of this process to bulk as opposed to defect relaxation.

As the ac probe field strength is increased, two observations have been made: (1) a very-low-frequency dielectric relaxation appears which increases in characteristic frequency as the field strength increases. This relaxation has been shown to be due to molecular reorientation at the surface of the cell. This relaxation is likely to be especially observable in cells as thin as ours ($2.7 \mu\text{m}$) and we expect its influence to become unobservable for the considerably thicker cells generally employed in studies of this type, and (2) the bulk molecular relaxation is still present but its behavior has been profoundly influenced by the larger ac probe field. The critical-like behavior near T_c is no longer observed, and the temperature-dependent behavior is similar to that observed in the dielectric-response measurements commonly reported for other liquid crystals. We have shown the dielectric strength of the bulk relaxation to increase linearly with the spontaneous polarization.

The behavior of the bulk relaxation at high ac probe levels can be described by the conventional relationship between spontaneous polarization, characteristic time, and viscosity. A few degrees below the phase transition the bulk viscosity obeys the expected Arrhenius behavior for a thermally activated process. At low temperatures the viscosity for the surface reorientation can be as much as an order of magnitude larger than that in the bulk. Measurements of the optical switching of a liquid crystal in thin cells in response to voltage pulses also indicate the existence of distinct surface and bulk reorientation processes. As found here, the reorientation at the surface is the slower process.¹² That study further indicates that the

surface switching is due to the movement of domain walls, which cannot be moved for small applied fields. This result is also corroborated in this study, in which we found the dramatic slowing down of the surface relaxation with decreasing ac signal level until it finally is either extremely slow, or absent, at low signal levels.

The difference in the behavior of the bulk liquid-crystal relaxation at the small- and large-signal levels is due to the fact that the small signal measures the response of the liquid-crystal molecules for small deviations around their equilibrium configuration. For a cell of this thickness this equilibrium position involves motion of the dipole near the position where it is pointing toward one electrode or the other. The dipoles do not "switch" their orientation all the way from one electrode to the other in the applied ac field: the optical response contrast to the sinusoidal applied voltage at the low-signal levels is also sinusoidal. At the 1-V applied level, the dipoles actually switch orientations from one electrode all the way to the other in the applied ac field, and thus the dielectric response is that characteristic of large deviations from the molecular equilibrium position: the optical contrast saturates for instantaneous voltages larger than approximately 0.7 V during the application of the sinusoidal voltage. This is why the large-signal data are successfully interpreted in terms of the kinds of analysis commonly applied to the response of ferroelectric liquid crystals to large pulsed fields.

The temperature dependence of the dielectric behavior of BOH8/MPOBC at the low applied signal level looks quite similar to that predicted for current models for the behavior of chiral smectic liquid crystals in the vicinity of the SmC^* to SmA transition.¹³⁻¹⁶ In those models, the dielectric constant increases in the SmA phase as the SmC^* phase is approached, with the enhancement given by

$$\delta\epsilon_A = 4\pi C^2 \chi^2 / [kq^2 + \alpha(T - T_c)] \quad (6)$$

due to the electroclinic or piezoelectric effect. This is also known as "soft-mode" behavior, and is based on the fact that in the A phase, where the long molecule axis (molecular director) is usually perpendicular to the smectic layers, fluctuations in the tilt angles of the molecules, similar to those occurring in the SmC^* phase, occur with longer and longer lifetimes as the SmC^* phase is approached. In Eq. (6), C is the linear-coupling coefficient between polarization and tilt; χ is the dielectric permittivity not influenced by the phase transition ($\epsilon_{\text{hf}} = 1 + 4\pi\chi$ in our notation); $k = k_{33} - \chi\mu^2$, where k_{33} is the bend nematic curvative elastic constant, and μ is the flexoelectric coupling constant; α is the soft mode susceptibility; and $q = 2\pi/p$, where p is the pitch of the helix.

In the SmC^* phase, the enhancement of the low-frequency dielectric constant is due to both piezoelectric and ferroelectric contributions

$$\delta\epsilon_c^* = 2\pi(C^2\chi^2/Kq^2 + C^2\chi^2/[Kq^2 + 2\alpha(T_c - T)]) \quad (7)$$

where the first term is the ferroelectric or "Goldstone mode" contribution, and the second term is the soft-mode contribution, which decreases in magnitude quickly as T

decreases away from T_c . The Goldstone-mode and soft-mode contributions to the dielectric response are best understood by considering the orientation of the molecular directors as being described by two terms,

$$\Theta = |\Theta| e^{i\Phi}, \quad (8)$$

where $|\Theta|$ is the projection of the molecular director on the plane of the layer (and therefore related to tilt angle) and Φ is the azimuthal angle of the molecular director about the normal to the planes. The soft-mode contributions are due to fluctuations in the molecular $|\Theta|$ and the Goldstone-mode contributions due to fluctuations in molecular Φ .

For our surface-stabilized sample, the helix of the liquid crystal is completely unwound; $p=0$, independent of temperature, and in Eqs. (6) and (7) $q=\infty$. The models are therefore not applicable in their literal form. However, we can assume that the liquid-crystal orientation in the applied electric field may still be described by fluctuations in $|\Theta|$ and Φ near the equilibrium molecular orientation. The models would still, therefore, predict that the enhanced dielectric response in the SmA phase is due to $|\Theta|$ fluctuations, and that in the SmC* phase is due to the sum of both $|\Theta|$ and Φ fluctuations near the phase transition, and solely Φ fluctuations at temperatures far from T_c .

Although the temperature dependence of ϵ_0 (Fig. 3) is entirely consistent with the theoretical models, they postulate that *two* relaxations contribute to the enhanced dielectric response in the SmC* phase. The $|\Theta|$ and Φ relaxations are said to coexist just below T_c , with the $|\Theta|$ relaxation decreasing in oscillator strength and increasing in characteristic frequency as temperature decreases, and the Φ relaxation maintaining temperature-independent oscillator strength and characteristic frequency. We observe the occurrence of only *one* relaxation, however, whose characteristic frequency varies continuously through the SmA to SmC* transition.

If the characteristic frequencies of the two relaxations are very similar, then they might be observed as an increase in the distribution of the characteristic frequencies rather than as two discrete relaxations. Such an increase, reflected in an increased α parameter, would be expected to occur in the SmC* phase between T_c and the temperature where ϵ_0 becomes a constant, for this material between 24.9°C and 22.3°C. An increase in α is in fact observed in the SmA phase very near T_c and for one temperature within the SmC* phase. (Far from T_c , $\alpha=0.1$ indicates a slight intrinsic broadening not associated with proximity to the phase transition.) It is highly unlikely that the increased broadening near T_c is associated with the occurrence of a second relaxation. Several other effects may be operating. (1) Thermal gradients on the order of hundredths of degrees within the sample will result in an increased α near T_c , as τ_0 is changing quickly with temperature in this region. (2) The molecular relaxation process near T_c may be particularly sensitive to a molecule's local environment; molecules closer to the surface, for instance, might relax at slightly different rates from those in the bulk. (3) The two-chemical mixture is likely to show phase-segregation effects in the vicinity of T_c , as a two-component mixture will not transform at a single temperature unless it is a eutectic.

It appears that our small-signal ac data can therefore not be interpreted in terms of distinct $|\Theta|$ and Φ relaxations. Rather, the best interpretation seems to be to attribute the enhanced response within both SmA and SmC* phases to a single process. This process is most likely the relaxation of Φ , the azimuthal angle of the molecular director, about its equilibrium configuration. This is commonly acknowledged to occur in SmC* phases, but may also occur in SmA phases, as fluctuations of the tilt of the molecules increase on approaching the SmC* phase; giving access to coupling of the electric field to the fluctuations of azimuthal angle which also may be occurring as T approaches T_c .

¹See, for instance, articles in *Ferroelectrics* **58** (1984).

²R. J. Cava, J. S. Patel, and E. A. Rietman, *J. Appl. Phys.* (to be published).

³G. W. Gray and J. W. Goodby, *Mol. Cryst. Liq. Cryst.* **37**, 157 (1956); J. S. Patel and J. W. Goodby (unpublished); J. W. Goodby, E. Chin, J. M. Geary, J. S. Patel, and P. L. Finn (unpublished). The abbreviation BOH8 stands for *S*-2''-methyl-(*n*-butyl) 4-(*n*-octylcarboxy)biphenyl 4'-carboxylate; MPOBC stands for *R*-1''-methyl-(*n*-propyl) 4-(*n*-octyloxy)biphenyl 4'-carboxylate.

⁴K. Miyasato, S. Abe, H. Takezoe, A. Fukuda, and E. Kuze, *Jpn. J. Appl. Phys.* **II 22**, L661 (1983).

⁵S. Havriliak and S. Negami, *J. Polym. Sci. C* **14**, 99 (1966).

⁶A. Levstik, B. Zeks, I. Levstik, R. Blinc, and C. Filipic, *J. Phys. (Paris) Colloq.* **40**, C3-303 (1979).

⁷D. P. Almond and A. R. West, *Solid State Ionics* **9,10**, 277 (1983).

⁸See, for instance, A. Sussman, *J. Appl. Phys.* **49**, 1131 (1978).

⁹K. Yoshino, M. Ozaki, H. Agawa, and Y. Shigeno, in Ref. 1.

¹⁰M. Glogarova, J. Pavel, and J. Fousek, *Ferroelectrics* in Ref. **55**, 117 (1984).

¹¹M. A. Handschy and N. A. Clark, *Ferroelectrics* **59**, 69 (1984).

¹²J. S. Patel, *Appl. Phys. Lett.* **47**, 1277 (1985).

¹³M. Glogarova, J. Fousek, L. Lejcek, and J. Pavel, *Ferroelectrics* **58**, 161 (1984).

¹⁴P. Martinot-Lagarde and G. Durand, *J. Phys. (Paris) Lett.* **41**, L43 (1980).

¹⁵R. Blinc and B. Zeks, *Phys. Rev. A* **18**, 740 (1978).

¹⁶Ph. Martinot-Lagarde and G. Durand, *J. Phys. (Paris)* **42**, 269 (1981).